A novel strategy to enhance kinetic energy models by considering channelization processes of PDCs

A. Aravena[1], R. Cioni[1], A. Bevilacqua[2], M. de' Michieli Vitturi[2], T. Esposti Ongaro[2], and A. Neri[2]

1 Dipartimento di Scienze della Terra, Universita di Firenze, Firenze, Italia.
2 Istituto Nazionale di Geofisica e Vulcanologia, Sezione di Pisa, Pisa, Italia.

February, 2020

Pyroclastic Density Currents

- Gravity-driven multiphase mixtures of hot particles (pyroclasts, lithics and gas) generated by collapsing eruptive collumns or volcanic domes.
- Several numerical models have been developed in order to assess the associated hazards.

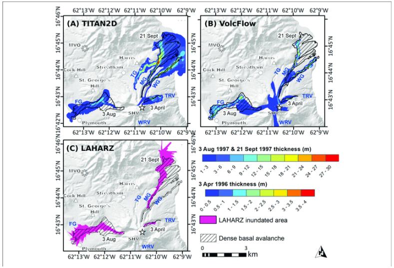

Figure 1. Numerical models used to assess the inundation area of PDCs (Ogburn and Calder, 2017).

Pyroclastic Density Currents: Numerical models

Roche et al. (2013) classified PDCs numerical models in four types:

(a) Kinetic models.
(b) Discrete elements models.
(c) Depth-averaged models.
(d) Multi-phase models.

Pyroclastic Density Currents: Kinetic models

- Kinetic models are based on the calculation of the kinetic energy in the flow front as a function of the distance traveled by the PDC.

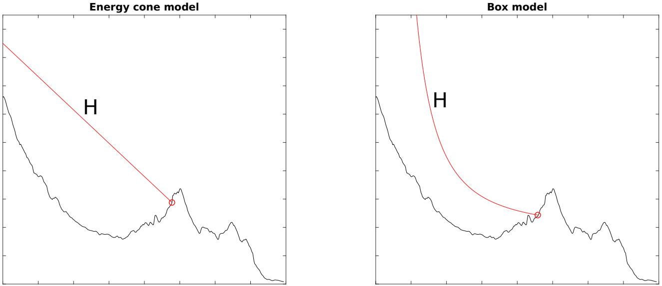

Figure 2. Function H of kinetic models.

Pyroclastic Density Currents: Energy cone model

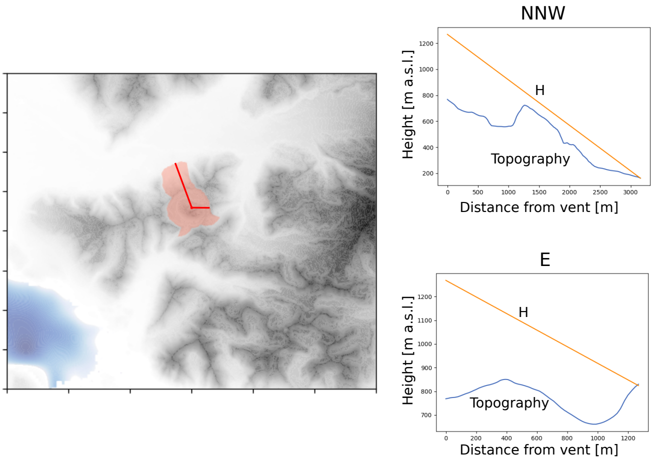

Figure 3. Example of application of the energy cone model.

Pyroclastic Density Currents: Energy cone model

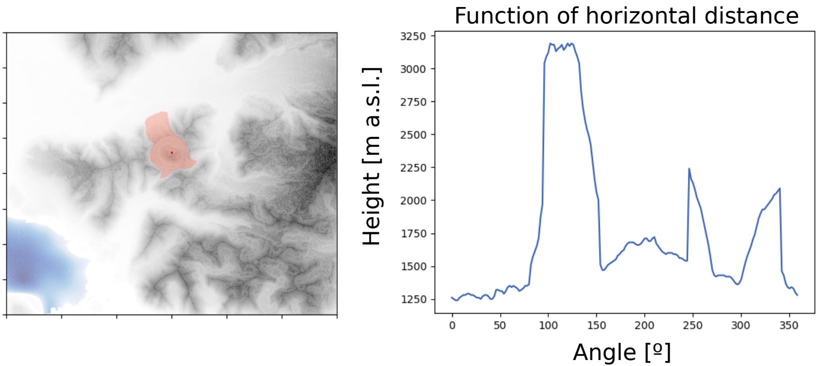

Figure 4. Example of application of the energy cone model.

Branching formulation

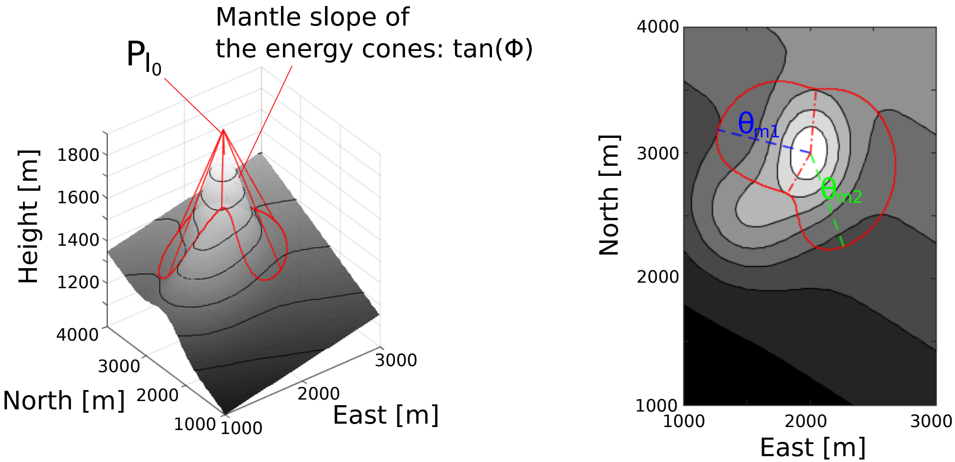

Figure 5. Example of application of the energy cone model.

Branching formulation

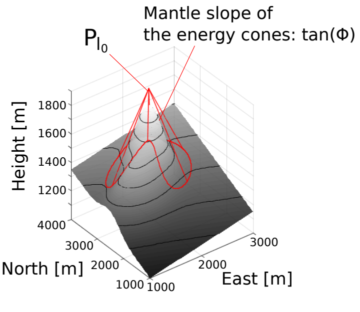

Figure 5. Application of the energy cone model.

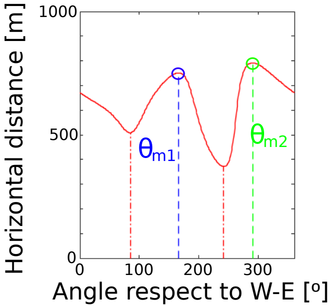

Figure 6. Function of horizontal distance.

Branching formulation

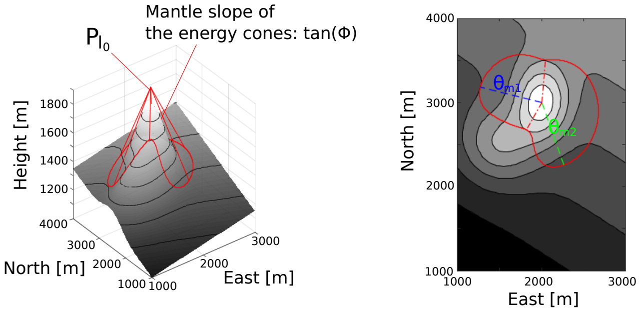

Figure 5. Energy cone model.

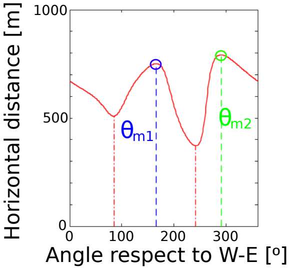

Figure 6. Function of horizontal distance.

(a) Vent position of energy cones.

(b) Mantle slope of energy cones.

(c) Apex height of energy cones.

Branching formulation

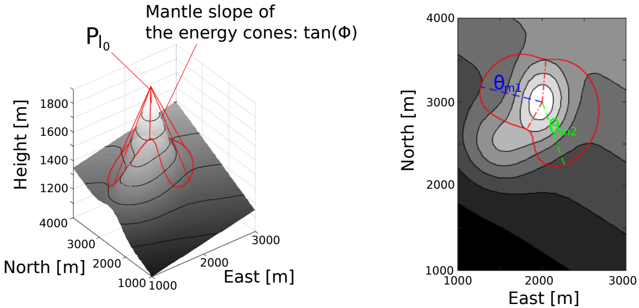

Figure 5. Energy cone model.

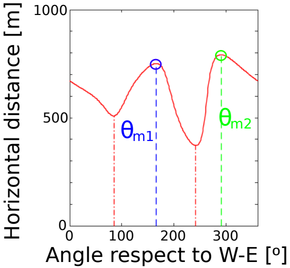

Figure 6. Function of horizontal distance.

(a) Vent position of energy cones.

$$P_m = (x_v + d(\theta_m)\cdot\cos(\theta_m), y_v + d(\theta_m)\cdot\sin(\theta_m)) \quad (1)$$

Branching formulation

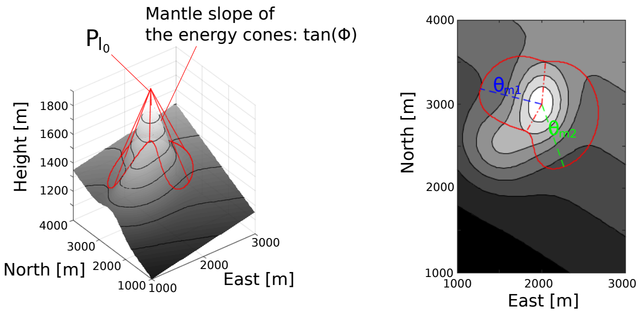

Figure 5. Energy cone model.

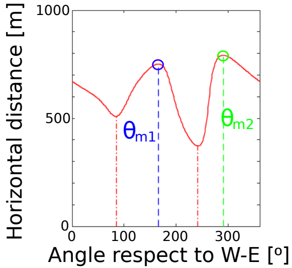

Figure 6. Function of horizontal distance.

(b) Mantle slope of energy cones.

Branching formulation

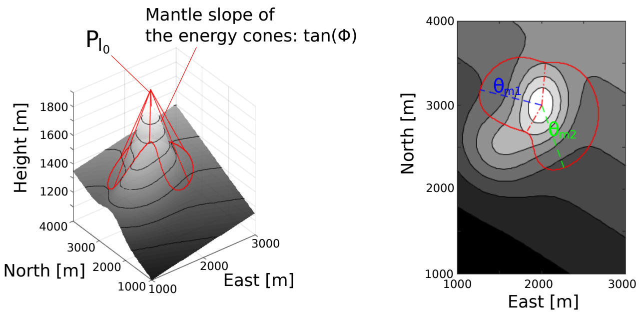

Figure 5. Energy cone model.

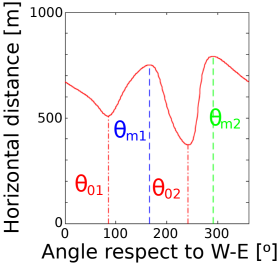

Figure 6. Function of horizontal distance.

(c) Apex height of energy cones.

$$E_r(\theta_o,\theta_m) \propto (d(\theta_m) - d(\theta_o)) \cdot \tan(\phi) \qquad (2)$$

Branching formulation

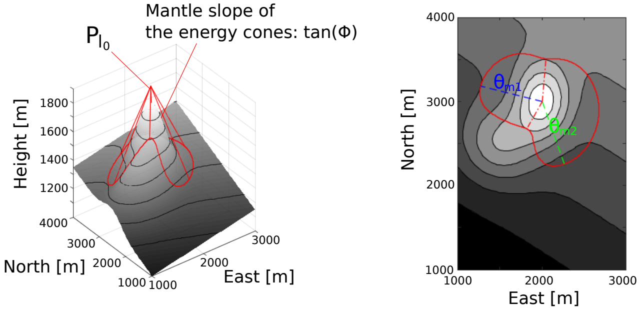

Figure 5. Energy cone model.

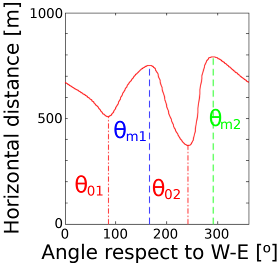

Figure 6. Function of horizontal distance.

(c) Apex height of energy cones.

$$H_m = \frac{1}{2\pi}\int_{\theta_1}^{\theta_2} (d(\theta_m) - d(\theta_o)) \cdot \tan(\phi) d\theta \qquad (3)$$

Branching formulation

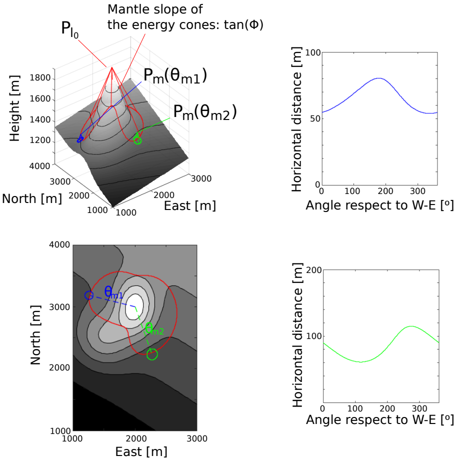

Figure 7. Branching formulation.

Branching formulation

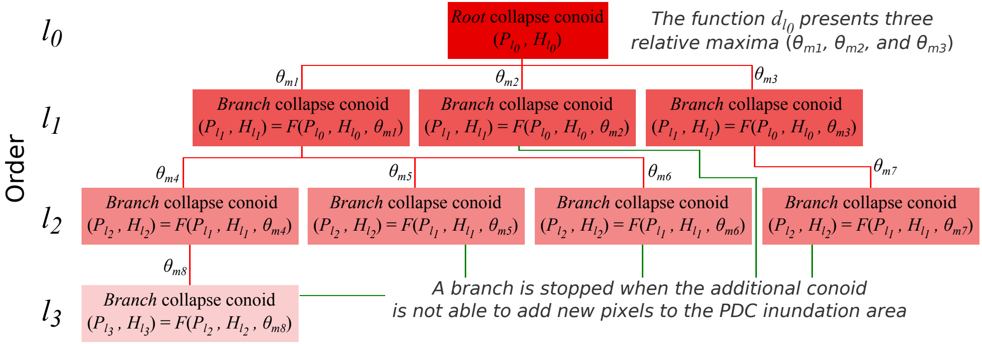

Figure 8. Structure of branching formulation.

Branching formulation: Example

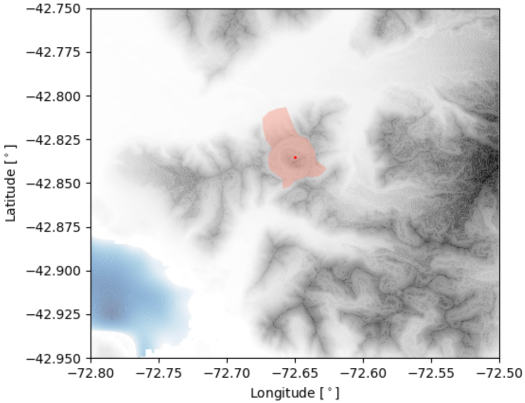

Figure 9. Branching formulation applied to Chaiten volcano ($l_{max} = 1$).

Branching formulation: Example

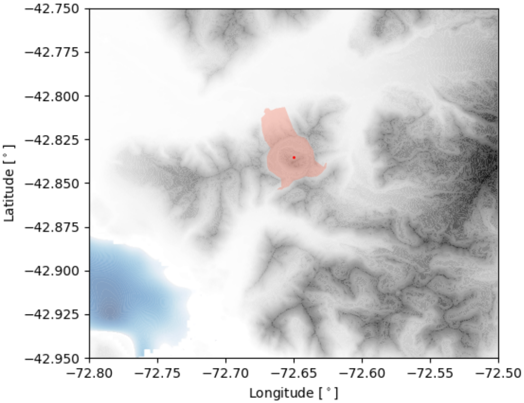

Figure 9. Branching formulation applied to Chaiten volcano ($l_{max} = 2$).

Branching formulation: Example

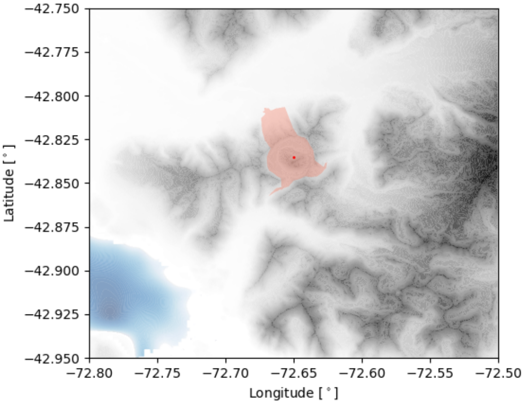

Figure 9. Branching formulation applied to Chaiten volcano ($l_{max} = 3$).

Branching formulation: Example

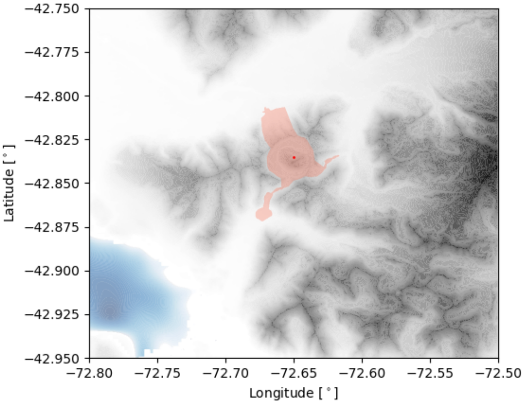

Figure 9. Branching formulation applied to Chaiten volcano ($l_{max} = 5$).

Branching formulation: Example

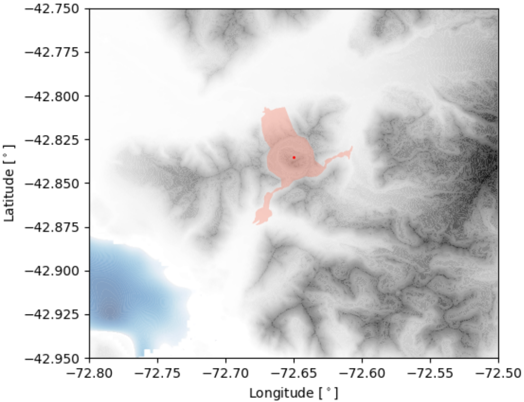

Figure 9. Branching formulation applied to Chaiten volcano ($l_{max} = \infty$).

Branching formulation: Example

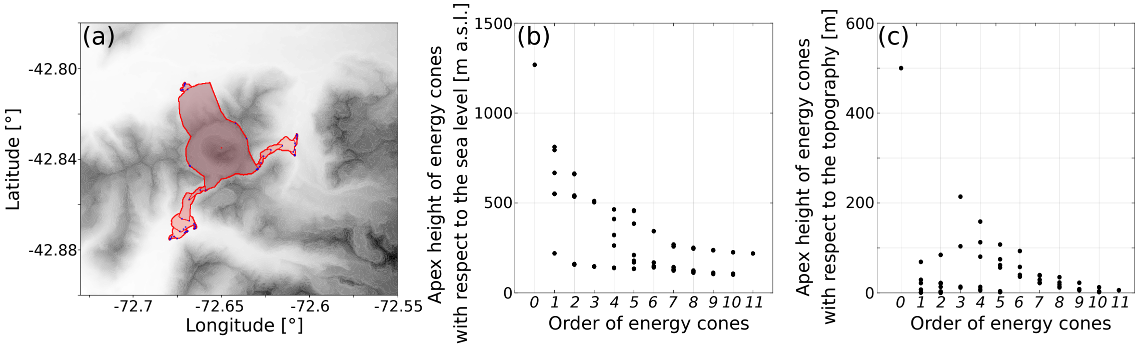

Figure 10. Branching formulation applied to Chaiten volcano ($l_{max} = \infty$).

Branching formulation: Probabilistic approach

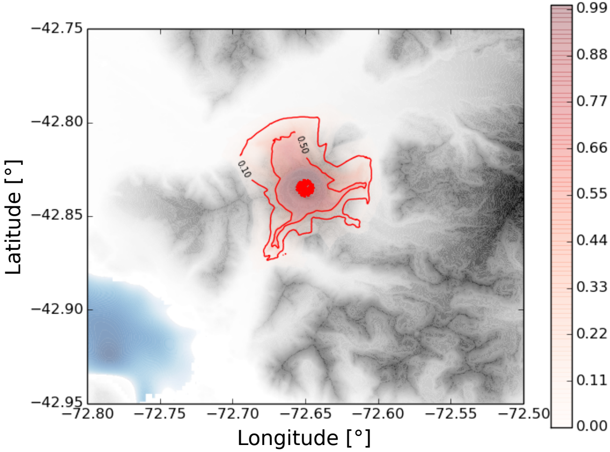

Figure 11. Branching formulation applied to Chaiten volcano.

Branching formulation: Probabilistic approach

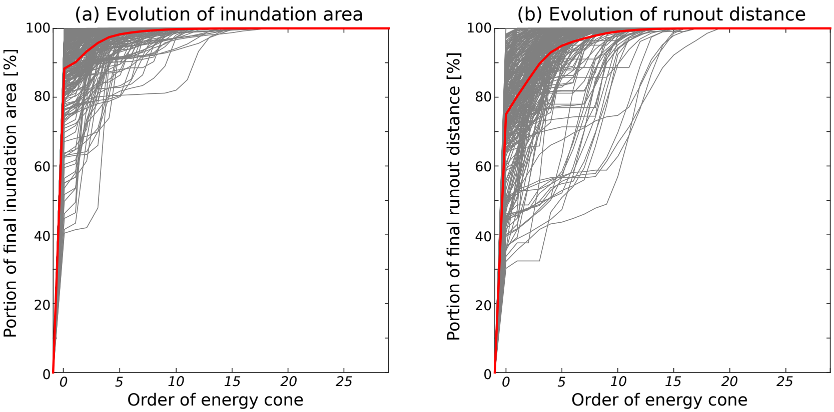

Figure 12. Branching formulation applied to Chaiten volcano.

Branching formulation: Probabilistic approach

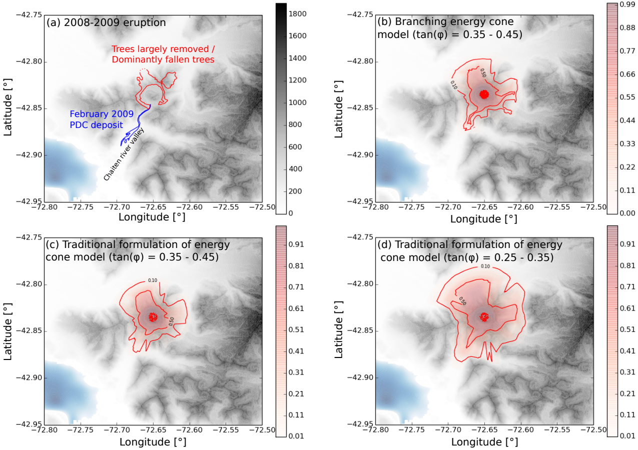

Figure 13. Branching and traditional formulation applied to Chaiten volcano.

Branching formulation: Probabilistic approach

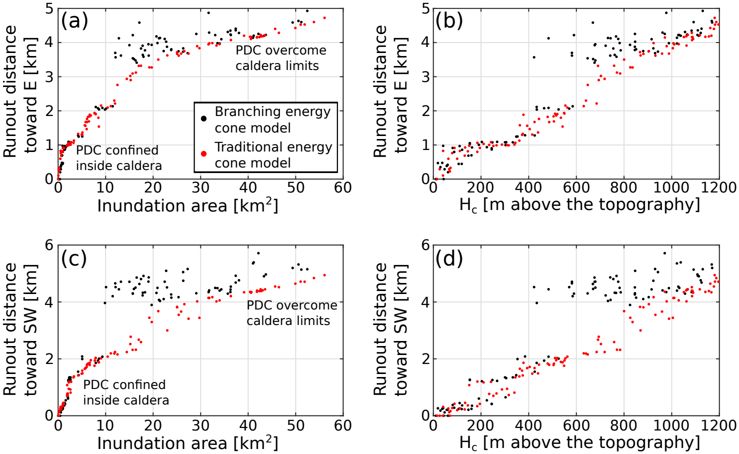

Figure 14. Branching and traditional formulation applied to Chaiten volcano.

Branching formulation: Comparison with IMEX_SfloW2D

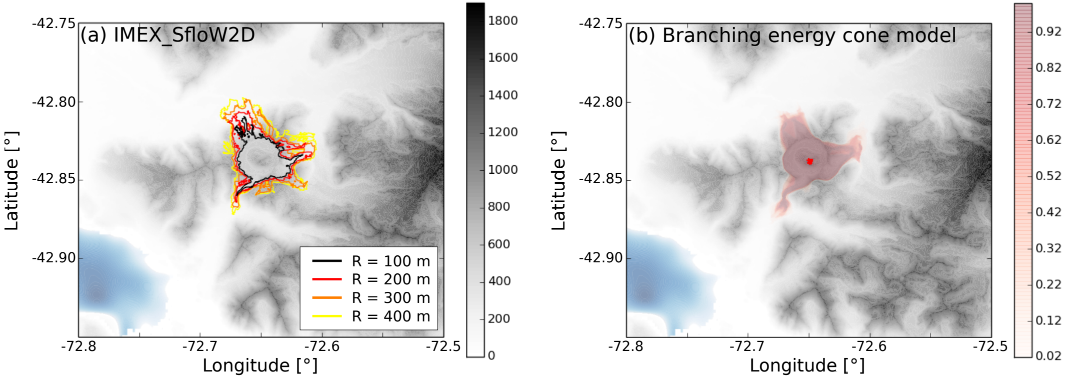

Figure 15. Branching formulation and IMEX_SfloW2D applied to Chaiten volcano.

Branching formulation: Peteroa volcano

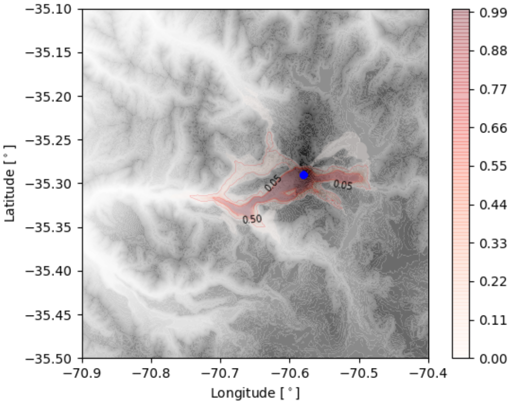

Figure 16. Branching formulation applied to Peteroa volcano.

Branching formulation: Fuego volcano

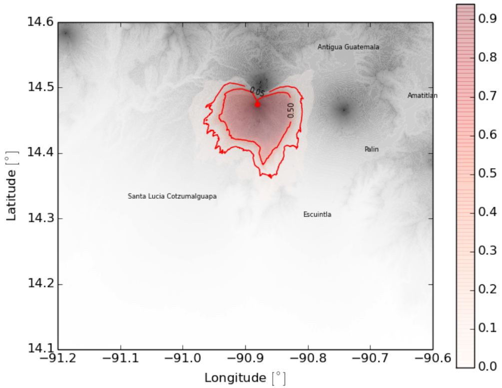

Figure 17. Branching formulation applied to Fuego volcano.

Branching formulation: Teide volcano

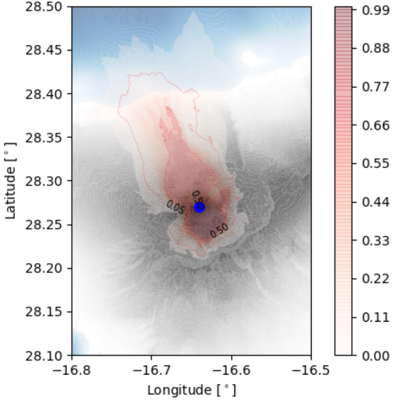

Figure 18. Branching formulation applied to Teide volcano.

Branching formulation: Citlaltepetl volcano

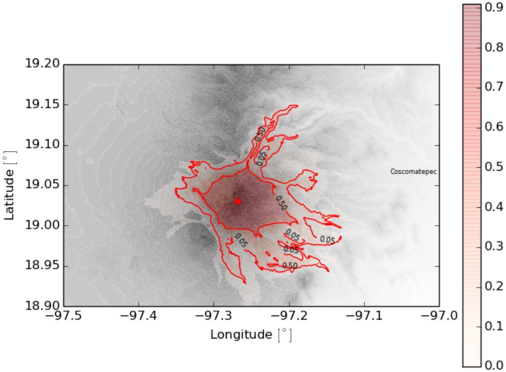

Figure 19. Branching formulation applied to Citlaltepetl volcano.

Branching formulation: Vesuvius volcano

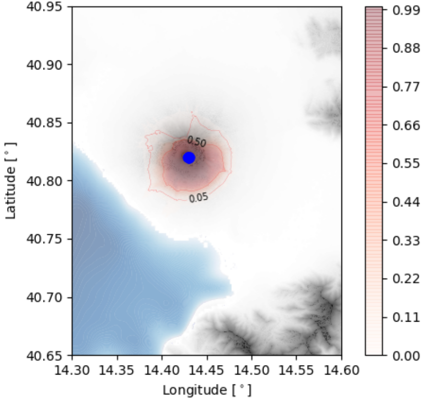

Figure 20. Branching formulation applied to Vesuvius volcano.

Branching formulation (Box model): Vesuvius volcano

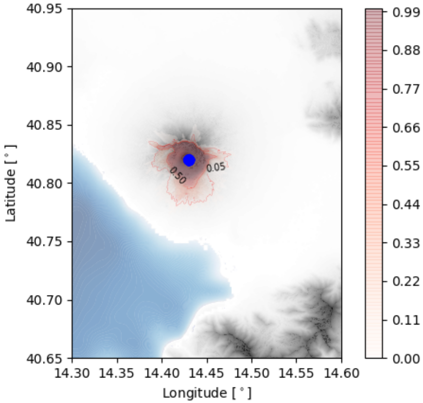

Figure 21. Branching formulation (box model) applied to Vesuvius volcano.

Concluding remarks

(a) We present a new strategy that allows improving kinetic models in order to consider flow channelization processes.

(b) Two widely used kinetic models were modified by applying this strategy. They are currently available in github (http://www.github.com/AlvaroAravena/ECMapProb for the energy cone model, and http://www.github.com/AlvaroAravena/BoxMapProb for the box model), including a user-friendly interface.

(c) We tested these branching formulations by comparing their results with those derived from the traditional formulations, with other numerical models, and with the area invaded during specific case studies.

(d) We show the capability of this strategy of improving the accuracy of kinetic models without adding new, unconstrained input parameters.

Gracias

Grazie

Thank you

References

Bevilacqua, A., A. Neri, M. Bisson, T. Esposti Ongaro, F. Flandoli, R. Isaia, M. Rosi, and S. Vitale (2017), The effects of vent location, event scale, and time forecasts on pyroclastic density current hazard maps at Campi Flegrei caldera (Italy), Frontiers in Earth Science, 5, 72.
de' Michieli Vitturi, M., T. Esposti Ongaro, G. Lari, and A. Aravena (2019), IMEX_SfloW2D 1.0: a depth-averaged numerical flow model for pyroclastic avalanches, Geoscientific Model Development, 12.
Dufek, J., T. Esposti Ongaro, and O. Roche (2015), Pyroclastic density currents: processes and models, in The Encyclopedia of Volcanoes, edited, pp. 617-629, Elsevier.
Lara, L. (2009), The 2008 eruption of the Chaiten Volcano, Chile: a preliminary report, Andean Geology, 36(1), 125-129.
Major, J., and L. Lara (2013), Overview of Chaiten Volcano, Chile, and its 2008-2009 eruption, Andean Geology, 40(2), 196-215.
Murcia, H., M. Sheridan, J. Macias, and G. Cortes (2010), TITAN2D simulations of pyroclastic flows at Cerro Machin Volcano, Colombia: Hazard implications, Journal of South American Earth Sciences, 29(2), 161-170.
Ogburn, S.E., and E.S. Calder (2017), The relative effectiveness of empirical and physical models for simulating the dense undercurrent of pyroclastic flows under different emplacement conditions, Frontiers in Earth Science, 5, 83.
Roche, O., J. Phillips, and K. Kelfoun (2013), Pyroclastic density currents, in Modeling Volcanic Processes: The Physics and Mathematics of Volcanism, edited, pp. 203-229.
Sheridan, M., and M. Malin (1983), Application of computer-assisted mapping to volcanic hazard evaluation of surge eruptions: Vulcano, Lipari, and Vesuvius, Journal of Volcanology and Geothermal Research, 17(1-4), 187-202.
Tadini, A., M. Bisson, A. Neri, R. Cioni, A. Bevilacqua, and W. Aspinall (2017), Assessing future vent opening locations at the Somma-Vesuvio volcanic complex: 1. A new information geodatabase with uncertainty characterizations, Journal of Geophysical Research: Solid Earth, 122(6), 4336-4356.
Tierz, P., L. Sandri, A. Costa, L. Zaccarelli, M. Di Vito, R. Sulpizio, and W. Marzocchi (2016a), Suitability of energy cone for probabilistic volcanic hazard assessment: validation tests at Somma-Vesuvius and Campi Flegrei (Italy), Bulletin of Volcanology, 78(11), 79.
Tierz, P., L. Sandri, A. Costa, R. Sulpizio, L. Zaccarelli, M. Di Vito, and W. Marzocchi (2016b), Uncertainty assessment of pyroclastic density currents at Mount Vesuvius (Italy) simulated through the energy cone model, Natural Hazard Uncertainty Assessment: Modeling and Decision Support, 223, 125-145.
Wadge, G., and M. Isaacs (1988), Mapping the volcanic hazards from Soufriere Hills Volcano, Montserrat, West Indies using an image processor, Journal of the Geological Society, 145(4), 541-551.